Nanotechnology **20** (2009) 075603 (6pp) doi:10.1088/0957-4484/20/7/075603

Catalyst-free nanowires with axial $In_xGa_{1-x}As$/GaAs heterostructures

Martin Heiß[1,2], Anders Gustafsson[6], Sonia Conesa-Boj[3], Francesca Peiró[3], Joan Ramon Morante[3,5], G Abstreiter[1], Jordi Arbiol[3,4], Lars Samuelson[6] and Anna Fontcuberta i Morral[1,2]

[1] Walter Schottky Institut, Technische Universität München, Am Coulombwall 3, D-85748 Garching, Germany
[2] Laboratoire des Matériaux Semiconducteurs, Institut des Matériaux, Ecole Polytechnique Fédérale de Lausanne, CH-1015 Lausanne, Switzerland
[3] EME/XaRMAE/IN^{2}UB, Departament d'Electrònica, Universitat de Barcelona, E-08028 Barcelona, CAT, Spain
[4] TEM-MAT, Serveis Cientificotècnics, Universitat de Barcelona, 08028 Barcelona, CAT, Spain
[5] IREC, Catalonia Institute for Energy Research, Josep Pla 2, 08019 Barcelona, CAT, Spain
[6] Solid State Physics, The Nanometer Consortium, Lund University, Box 118, Lund S-221 00, Sweden

E-mail: anna.fontcuberta-morral@epfl.ch

Received 4 November 2008, in final form 11 December 2008
Published 26 January 2009
Online at stacks.iop.org/Nano/20/075603

Abstract
Self-catalyzed growth of axial $In_xGa_{1-x}As$/GaAs heterostructures has been realized by molecular beam epitaxy. The growth of the wires is achieved from gallium/indium alloy droplets that are nucleated *in situ*. By variation of the In/Ga beam flux during the growth it was possible to vary the effective indium content up to $x = 5\%$, as deduced from photoluminescence measurements. We have analyzed the dependence of the alloy concentration on the growth conditions and present a simple model for the growth. The heterostructures grown with the method presented were spatially mapped along the wires with confocal microphotoluminescence and cathodoluminescence. It was found as expected that the emission of GaAs/$In_xGa_{1-x}As$/GaAs heterostructures is localized. This work is important for the use of an external catalyst-free growth of complex axial heterostructures and related opto-electronic devices that facilitates its possible integration in the device or system fabrication processes.

(Some figures in this article are in colour only in the electronic version)

1. Introduction

Semiconductor nanowires are of high interest as potential building blocks for future optical and electronic devices, such as high mobility transistors, bright LEDs and solar cells [1–5]. Avoiding the use of external catalysts such as gold as a seed for nucleation and growth of the nanowires has been and is a crucial issue. It is important both for the future application of nanowires in industrial applications, but also in fundamental research where high purity of the materials used enables investigations of new phenomena [6, 7]. Very low concentrations of metal impurities such as gold harm the semiconductor properties because they introduce deep levels in the band gap [8]. Due to this fact, nanowire growth has been achieved by the use of alternative metals such as aluminum, titanium and copper—that dope or have much lower solubility—or by simply avoiding the use of a catalyst [9–13]. Recently, we have demonstrated a method for gallium-assisted nucleation and growth of gallium arsenide nanowires [14, 15]. In the present work we show how this mechanism used for binary wires can be extended to the ternary $In_xGa_{1-x}As$ material system, and to the related heterostructures. This certainly opens up the possibility of fabricating more complex nanowire structures and devices. While several reports on axial nanowire heterostructures grown with MOCVD using a gold catalyst already exist [16–19], to date results on catalyst-free growth of heterostructures have rarely been reported.

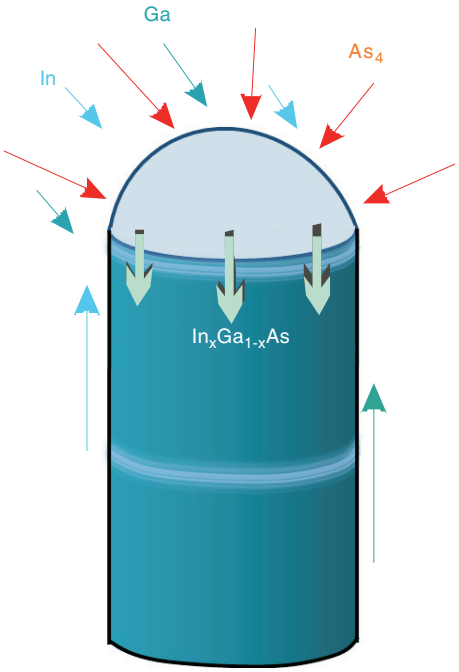

Figure 1. Schematic of the growth principle for the formation InGaAs nanowires from an InGa alloy droplet.

2. Experimental details

The synthesis was carried out in a GenII molecular beam epitaxy (MBE) machine. GaAs (111)B oriented substrates covered with 40 nm SiO_2 were used. Prior to introducing the substrates in the MBE, the oxide was etched down to 10 nm with a diluted buffered HF solution (ammonium fluoride etch solution (91-9):deionized water = 1:2) [14]. During the growth the substrate temperature was kept at 903 K. The gallium rate and the arsenic beam flux were kept respectively at 0.25 Å s^{-1} and 8.8 × 10^{-7} mbar. Several growth runs were performed using indium beam flux ratios corresponding to a nominal planar growth rate of 0.088–0.1 Å s^{-1}. We report on the growth of $In_xGa_{1-x}As$ nanowires and GaAs nanowires in which $In_xGa_{1-x}As$ sections have been included by opening the In cell at intervals during the growth. The wires include homogeneous GaAs and $In_xGa_{1-x}As$ nanowires, as well as GaAs nanowires with $In_xGa_{1-x}As$ segments of varying lengths.

The structure of the nanowires, their indium content and optical properties were studied by transmission electron microscopy (TEM), Energy dispersive x-ray spectroscopy (EDX), photoluminescence (PL) and cathodoluminescence spectroscopy (CL). PL and CL were measured respectively at 4.2 and 9 K using respectively a cryogenic confocal microscope and an adapted scanning electron microscope. For the TEM measurements, the wires were mechanically removed from the substrate and transferred with an n-hexane droplet to a holey-carbon grid. For the CL and PL measurements, the nanowires were transferred to a silicon substrate by just gently rubbing the surfaces of the two samples together.

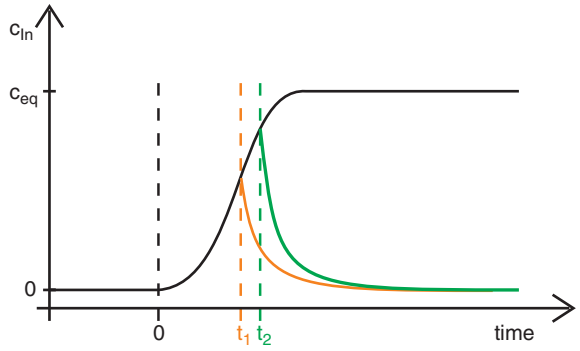

Figure 2. Schematic time dependence of indium concentration of precipitated InGaAs material for transition to equilibrium (black) and indium incubation times t_1 (orange) and t_2 (green). $t = 0$ corresponds to the moment of opening the indium cell.

3. Experimental results

3.1. Growth principle

As we have demonstrated in the past, it is possible to obtain GaAs nanowires with MBE by using gallium as the nucleation seed instead of gold, by growing under gallium rich conditions. We have shown that, in contrast to what is observed in thin film epitaxy, the growth rate of the nanowires is controlled by the arsenic beam flux. Gallium forms droplets, which gather and alloy with the arsenic molecules forming GaAs underneath the droplet [14]. By adding indium during the growth, this element may incorporate in the droplet forming an alloy with gallium. If arsenic alloys with the both components of the droplet, this leads into the formation of $In_xGa_{1-x}As$ nanowires. The indium content of the final alloy will depend on the complex metallurgy of indium and gallium at the droplet stage and on the thermodynamics of the alloy in the solid state [20]. A schematic drawing of this principle is shown in figure 1. More important is the kinetics of incorporation of indium both at the droplet and nanowire level, indicated in figure 2. Let us assume that, after having started the growth of GaAs nanowires, the indium flux is turned on. Due to the low arsenic beam flux and the high temperature, almost no indium can be incorporated directly on the substrate or nanowire facets and it will start to diffuse to the gallium droplet, forming an indium–gallium alloy. After a certain characteristic time τ, the droplet will reach the equilibrium concentration of both metals. During this incubation period, the nanowire continues to grow by the association of arsenic with both gallium and indium present in the droplet. This means that the indium content of the $In_xGa_{1-x}As$ nanowires will gradually increase along the growth axis and then saturate as the droplet has achieved the equilibrium concentration. In a similar way, once the indium source is turned off, the In–Ga droplet will gradually become depleted of indium. As it will be shown in the following, the temporal response of the indium incorporation will be especially important in cases of axial heterostructures.

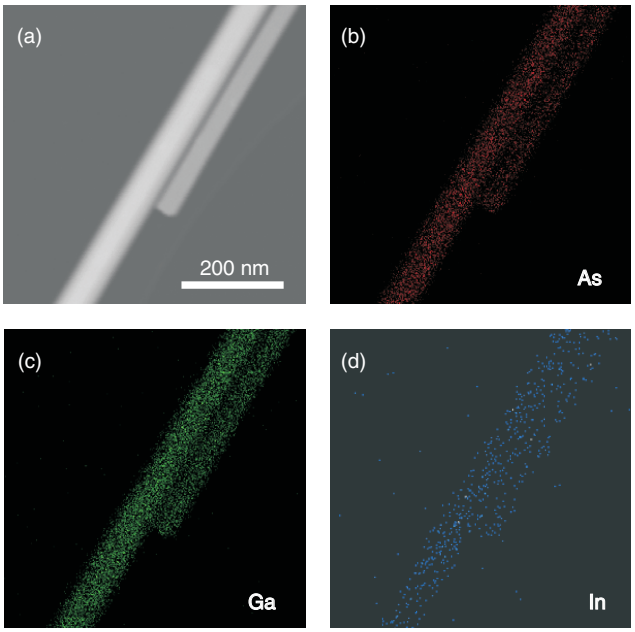

Figure 3. (a) TEM image of two nanowires annexed to each other; EDX elemental analysis corresponding to As (b), Ga (c) and indium (d).

3.2. Structural analysis of the indium incorporation

In this section we would like first to confirm the incorporation of indium in the nanowires, as this is the prerequisite for more complex structures. For that, we analyze 3 μm long nanowires that have been obtained with the indium and gallium source open during the entire growth, with an indium rate of 0.088 Å s^{-1} and Ga of 0.2 Å s^{-1}. The result should indicate the equilibrium indium concentration, given the temperature, gallium and indium rates.

The presence of indium and the concentration in an $In_xGa_{1-x}As$ alloy can be measured by energy dispersive x-ray analysis (EDX). By combining EDX with scanning TEM (STEM), it is possible to realize maps of the elements composing a sample. Figure 3(a) corresponds to the TEM image of two nanowires next to each other. The element analysis realized with EDX is shown in figures 3(b)–(d). As it can be seen, the elements arsenic, gallium and indium are detected in the whole length of the nanowires. It is also clear that the presence of indium is sensibly inferior to the presence of gallium. Due to the small amount of indium with respect to the gallium, it is difficult to quantify the content in the present alloy.

High resolution TEM has also been realized, for determination of the crystal structure. An overview TEM micrograph of two $In_xGa_{1-x}As$ nanowires is presented in figure 4(a). The nanowires present diameters of about 60 nm. The crystal structure was analyzed in detail along the nanowires. The wires grow along the $[1\bar{1}1]$ axis and present a zinc blende structure, with twins perpendicular to the growth direction spaced between 20 and 30 nm. The presence of twins along the $[1\bar{1}1]$ planes has been commonly observed in III–V and even in group IV nanowires [15, 21–23]. High Resolution TEM micrographs of two sections one of the wires in figure 4(a) are shown in figures 4(b) and (c). Figure 4(b) corresponds to a section at the end of the nanowire, while figure 4(c) corresponds to the middle. Notice that in the middle part of the nanowire the surface present a slight roughening not observed previously in our pure GaAs nanowires [15].

3.3. Axial heterostructures

GaAs nanowires were grown, with $In_xGa_{1-x}As$ sections of different lengths by opening the indium source at intervals of different duration. All nanowires were passivated *in situ* by growing a planar layer of 3 nm GaAs homogeneously on all the facets. Switching to radial growth is achieved by reducing the substrate temperature to 760 K and increasing the As_4

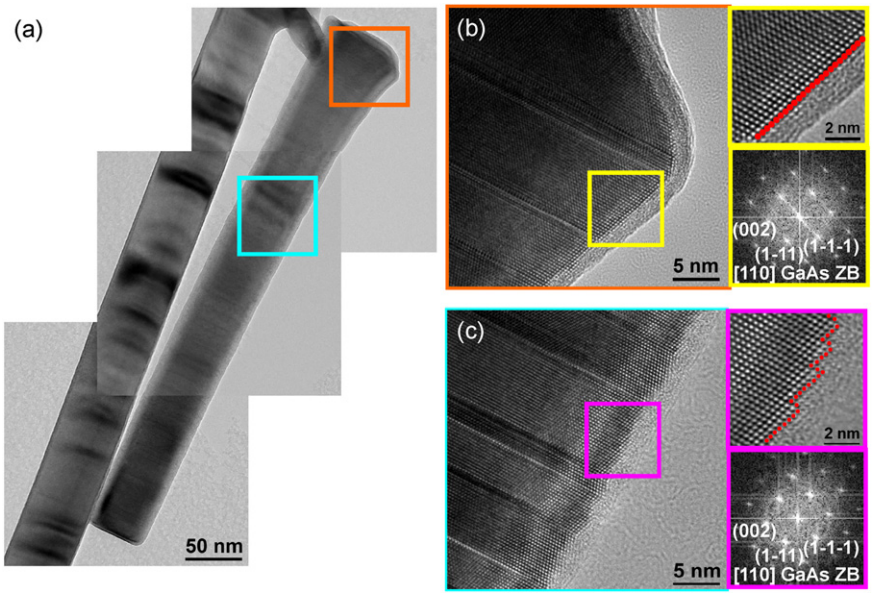

Figure 4. (a) TEM micrograph of InGaAs nanowires. ((b), (c)) High resolution TEM sections of the nanowires.

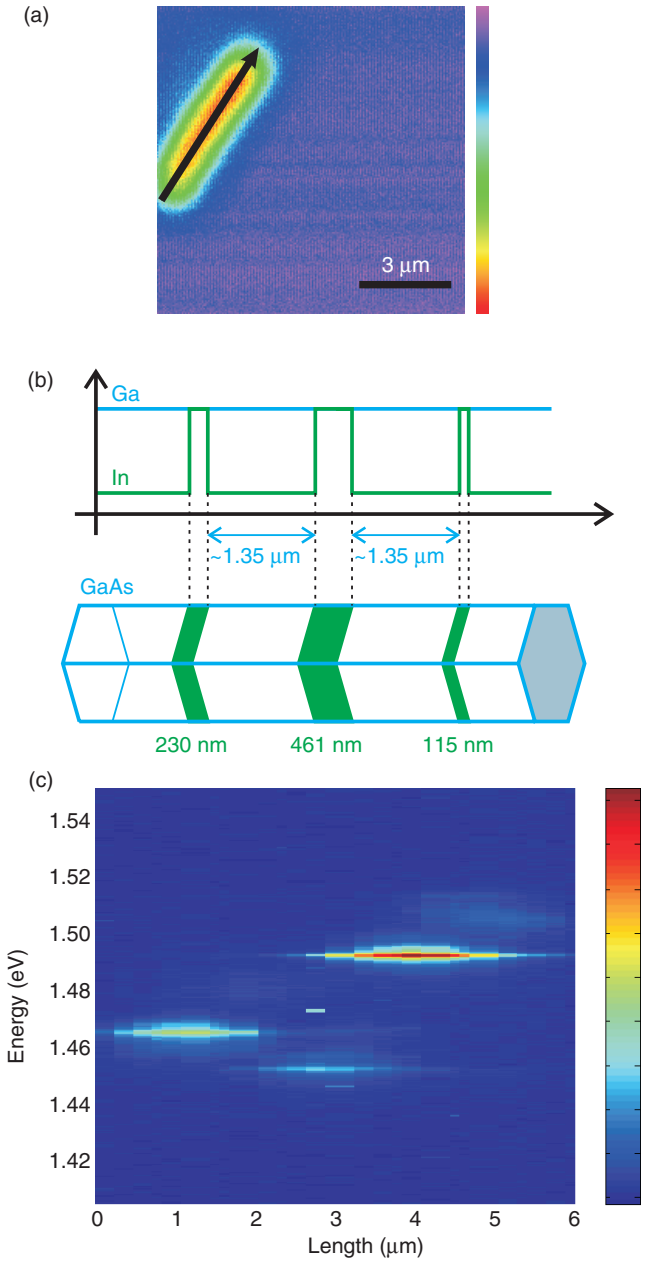

Figure 5. (a) Confocal microscopy reflectivity mapping showing the presence of a single nanowire lying on a SiO_2 substrate; (b) schematic of the nanowire layout as expected from the growth protocol; (c) 4.2 K μ-Photoluminescence mapping scan of a single nanowire along the nanowire axis as indicated by the arrow in (a).

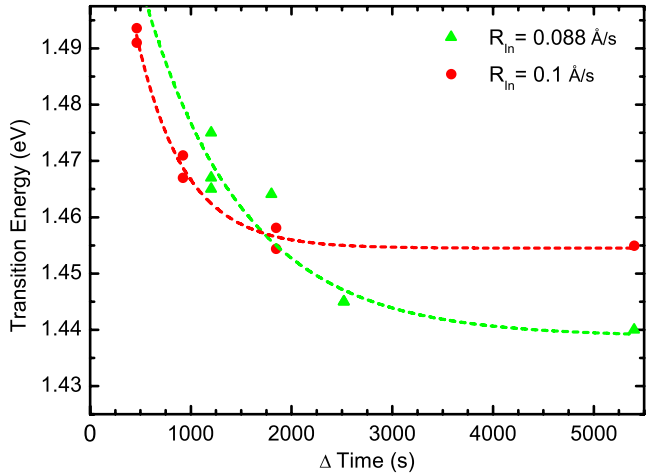

Figure 6. Dependence of measured photoluminescence emission on the opening time of the indium cell during growth for two different indium deposition rates of 0.1 and 0.088 Å s^{-1}.

pressure to 5×10^{-5} mbar. For the investigation of the optical properties, the nanowires were first transferred to a piece of silicon substrate. In order to find isolated single nanowires, the surface was first scanned with the optical confocal microscope in reflectivity mode. An example is shown in figure 5(a). The decrease in reflectivity can be clearly related to the presence of a nanowire. After finding an isolated nanowire a scan of the surface in spectroscopic mode is performed. This allows us to map regions with different photoluminescence emission characteristics. As an example, we present a nanowire with three $In_xGa_{1-x}As$ sections. The growth process is schematized in figure 5(b). The first section started after growth of 500 nm of the GaAs. The indium cell was open for 920 s, which corresponds typically to the growth of 230 nm. Then, the GaAs nanowire growth proceeded during 1.35 μm grown before the In cell was open for a second time, during 1844 s (equivalent to 461 nm). Again, after growing a length of 1.35 μm with only Ga supply, the In cell was opened for 460 s, equivalent to 115 nm. In figure 5(c) an example of spectroscopic scan of one of these nanowires. The light emission is basically located in three different spots of the wire, which can be attributed to the sections containing $In_xGa_{1-x}As$. Moreover, the energy position of the emitted light differs from section to section and decreases as a function of the time the In shutter was open. Indeed, an emission at 1.495 eV is observed when the indium was open for the shortest time, while an emission at 1.465 and 1.455 eV is observed for 920 and 1844 s opening times.

In order to better understand the dynamics of the incorporation of indium in the growth, more nanowires were synthesized with $In_xGa_{1-x}As$ sections that varied from 340 to 5400 s corresponding to 85 to 1350 nm long segments. This was realized for two different In rates: 0.088 and 0.1 Å s^{-1}. The optical properties of the resulting nanowires were investigated by PL at 4.2 K. The lowest transition energy measured for the GaAs/$In_xGa_{1-x}As$/GaAs heterostructures fabricated for different In opening time is plotted in figure 6. The transition energy clearly decreases as the indium opening time is increased, consistent with an increase of the indium content. Additionally, increasing the indium rate from 0.088 to 0.1 Å s^{-1} also leads to a higher incorporation of indium in the nanowire. Even higher rates were also tried, but this led into a less reproducible growth. We believe this is due to the complex In–Ga mixing thermodynamics [20]. The characteristic times for indium incubation deducted by a exponential decay fit are $\tau = 997$ s for the 0.1 Å s^{-1} indium rate, with a saturation of the PL signal at 1.439 eV, and $\tau = 475$ s for the 0.088 Å s^{-1} with a saturation of the PL signal at 1.455 eV. These measurements are in clear agreement with our model of the indium incorporation, as sketched in

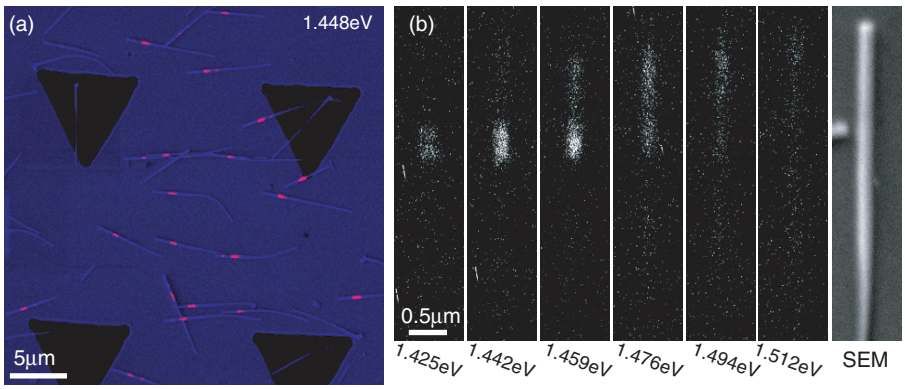

Figure 7. (a) Color-coded composite image of an area of the sample containing several nanowires, where red is a CL image and blue is the corresponding SEM image. The dark triangles are markers on the surface. The red lines show the emission from, and thereby the location of the segments. (b) SEM image and a set of monochromatic CL images of a single nanowire, growth direction is up. The intensity scale is the same for all the images showing a 500 nm long segment emitting at about 1.45 eV, and possibly an In contamination above the InGaAs segment.

figure 2 and correspond to an indium equilibrium concentration of 5.1% for 0.1 Å s^{-1} rate and 4.1% for 0.88 Å s^{-1} indium rate.

Finally, we report on spatially and spectrally resolved CL imaging performed at 9 K. The measurements were performed in a dedicated scanning electron microscope (SEM), where the electron beam is used to excite luminescence. The spatial resolution of CL imaging can be well below 100 nm, governed by the size of the electron beam and the spread of the beam electrons inside the sample. As the spatial resolution comes from the finite size of the excitation, the resolution can be reduced by diffusion of the excitation inside the sample. The experiments were performed with an acceleration voltage of 5 kV and a probe current of 50 pA. The luminescence was passed through a monochromator with a spectral resolution of 10 nm.

We investigated GaAs nanowires with one $In_xGa_{1-x}As$ section towards the top. First approximately 10 μm long GaAs nanowires were grown at a high growth rate at an increased As pressure of 3.5×10^{-6} mbar. Subsequently the As pressure was reduced to 8.8×10^{-7} mbar, and a length of 390 nm GaAs section was grown. This was followed by the growth with the indium cell open during 2519 s, which should correspond to a nanowire segment of 630 nm. Finally, the last 500 nm of GaAs were grown after closing the In cell again. At last, the nanowire facets were capped with a 3 nm GaAs layer.

We recorded sets of monochromatic CL images and corresponding SEM images of a number of nanowires. A typical image of the main $In_xGa_{1-x}As$ emission is shown in figure 7(a), together with a set of images of a single nanowire in figure 7(b). In the case of these nanowires, the emission intensity decreased with electron beam exposure, so the images were recorded with a minimum of beam exposure. The present sample consisted of nanowires transferred to a gold-coated silicon substrate. Figure 7(a) shows a color-coded image, where the SEM image is in blue and the CL image recorded at 1.448 eV is red. This is the main emission of the $In_xGa_{1-x}As$ segment. The apparent segment size is about 500 nm. The image also indicates that the GaAs above the InGaAs segment contains some In, as evidenced by the weak emission above the segment in the 1.476 eV image. Due to the diffusion of the excitation in the nanowire, it is not possible to determine if there are any variations in In content inside the segment.

4. Conclusions

We have studied the formation of $In_xGa_{1-x}As$ heterostructures in nanowires by catalyst-free molecular beam epitaxy. The incorporation of In has been proven by EDX Spectroscopy. The dynamics of In incorporation for the fabrication of $In_xGa_{1-x}As$/GaAs heterostructures has been studied, indicating that a transition time in the order of 1000 s is needed for reaching the maximum concentration of indium in the $In_xGa_{1-x}As$ alloy. Finally the spatial localization of GaAs/$In_xGa_{1-x}As$/GaAs heterostructures has been studied by optical confocal photoluminescence and spectroscopic cathodoluminescence. Spatially resolved maps of the emission have been obtained. This work is important for the further development of catalyst-free nanowire heterostructures and related devices.

Acknowledgments

The authors would like to thank D Grundler, T Garma, D Spirkoska, and M Bichler for their experimental support. This research was supported by Marie Curie Excellence Grant 'SENFED', and the DFG excellence initiative Nanosystems Initiative München and SFB 631. This work was also supported in part by the Swedish Foundation for Strategic Research (SSF), the Swedish Research Council (VR) and the Knut and Alice Wallenberg Foundation.

References

[1] Lu W, Xiang J, Timko B P, Wu Y and Lieber C M 2005 *Proc. Natl Acad. Sci.* **102** 10046–51
[2] Samuelson L, Björk M T, Deppert K, Larsson M, Ohlsson B J, Panev N, Persson A I, Sköld N, Thelander C and Wallenberg L R 2004 *Physica* E **21** 560–7
[3] Guichard A, Barsic D, Sharma S, Kamins T and Brongersma M 2006 *Nano Lett.* **6** 2140–4

[4] Schmidt V, Riel H, Senz S, Karg S, Riess W and Gösele U 2006 *Small* **2** 85–8
[5] Maiolo J, Kayes B, Filler M, Putnam M, Kelzenberg M, Atwater H and Lewis N 2007 *J. Am. Chem. Soc.* **129** 12346–7
[6] Klitzing K v, Dorda G and Pepper M 1980 *Phys. Rev. Lett.* **45** 494–7
[7] Wegscheider W, Schedelbeck G, Abstreiter G, Rother M and Bichler M 1997 *Phys. Rev. Lett.* **79** 1917–20
[8] Collins C B, Carlson R O and Gallagher C J 1957 *Phys. Rev.* **105** 1168–73
[9] Arbiol J, Kalache B, i Cabarrocas P R, Morante J R and Fontcuberta i Morral A 2007 *Nanotechnology* **18** 305606
[10] Wang Y, Schmidt V, Senz S and Gosele U 2006 *Nat. Nanotechnol.* **1** 186–9
[11] Kamins T I, Williams R S, Basile D P, Hesjedal T and Harris J S 2001 *J. Appl. Phys.* **89** 1008–16
[12] Mandl B, Stangl J, Martensson T, Mikkelsen A, Eriksson J, Karlsson L, Bauer G, Samuelson L and Seifert W 2006 *Nano Lett.* **6** 1817–21
[13] Fontcuberta i Morral A, Spirkoska D, Arbiol J, Heigoldt M, Morante J R and Abstreiter G 2008 *Small* **4** 899–903
[14] Colombo C, Spirkoska D, Frimmer M, Abstreiter G and Fontcuberta i Morral A 2008 *Phys. Rev.* B **77** 155326
[15] Fontcuberta i Morral A, Colombo C, Abstreiter G, Arbiol J and Morante J R 2008 *Appl. Phys. Lett.* **92** 063112
[16] Björk M, Thelander C, Hansen A, Jensen L, Larsson M, Wallenberg L and Samuelson L 2004 *Nano Lett.* **4** 1621–5
[17] Tchernycheva M, Cirlin G, Patriarche G, Travers L, Zwiller V, Perinetti U and Harmand J C 2007 *Nano Lett.* **7** 1500–4
[18] Ouattara L, Mikkelsen A, Sköld N, Eriksson J, Knaapen T, Cavar E, Seifert W, Samuelson L and Lundgren E 2007 *Nano Lett.* **7** 2859–64
[19] Verheijen M, Immink G, de Smet T, Borgstrom M and Bakkers E 2006 *J. Am. Chem. Soc.* **128** 1353–9
[20] Shen J Y and Chatillon C 1990 *J. Cryst. Growth* **106** 543–52
[21] Johansson J, Karlsson L S, Svensson C P T, Martensson T, Wacaser B A, Deppert K, Samuelson L and Seifert W 2006 *Nat. Mater.* **5** 574–80
[22] Davidson F M, Lee D C, Fanfair D D and Korgel B A 2007 *J. Phys. Chem.* C **111** 2929–35
[23] Arbiol J, Fontcuberta i Morral A, Estradé S, Peiró F, Kalache B, i Cabarrocas P R and Morante J R 2008 *J. Appl. Phys.* **104** 064312